REVISTA MATÉRIA V.31
ISSN 1517-7076 articles e20250844, 2026

3D evaluation of the use of steel slag in road layers as a sustainable soil improvement method

Mürüvet Özsoy[1], Nihat Sinan Işık[2], Seyhan Fırat[2]

[1]Aksaray University, Department of Civil Technologies. 68100, Aksaray, Türkiye.
[2]Gazi University, Faculty of Technology, Department of Civil Engineering. 06560, Çankaya, Ankara, Türkiye.
e-mail: munluozsoy@aksaray.edu.tr, nihatsinan@gazi.edu.tr, sfirat@gazi.edu.tr

ABSTRACT

The infrastructure layers of the highways must meet expectations both technically and economically. These layers that are not constructed properly cause deformations on the road surface. Steel slag should be preferred to reduce these deformations, increase the use of recycled materials worldwide, and create a sustainable system. For this purpose, the vertical deformation response of the flexible superstructure utilizing steel slag under dynamic wheel loads was analyzed numerically using the 3D FEM approach, in this study. Axle loads were applied considering the heavy vehicle tire layout plan and subjected to cyclic loading. The effect on the vertical settlement of the road was evaluated for four different sections defined using steel slag in the base and subbase layers. The axle load was applied to the determined wheel loading areas in loading steps throughout the cycle time, which was determined depending on the speed of the heavy vehicle and the tire dimensions. According to the results of the numerical analysis, the engineering performance of the sections with steel slag was better. Thus, innovative and sustainable approaches such as using steel slag aggregates instead of natural aggregates in the base and subbase layers of the highway were proposed.

Keywords: Soil stabilization; Deformation; Finite element methods; Roads & highways; Steel slag.

1. INTRODUCTION

In addition to the economic development of countries, the existence of efficient transportation networks is especially important in terms of increasing socio-cultural interactions. Basically, transportation types are grouped under three main headings: Highways, Seaways, and Airways. While it was reported that road transport was preferred by 52% in freight transport in the EU in 2019, maritime transport constituted 28.9%, rail transport constituted 12%, and air transport constituted only 0.1% of the total. Inland waterways and oil pipelines also make up the other percentage in this distribution [1]. From this point of view, highways are one of the most preferred modes of transportation worldwide.

The number of vehicles on the highway changes depending on several factors such as days, months, and years. Despite changes in the number of vehicles, damage to road structures exposed to repeated traffic loads is expected to continue to increase. The stresses created by moving wheel loads in the road structure are idealized as shown in Figure 1. Considering the passage of wheels over the road surface, there is a compression on the pavement surface in direct contact with the wheel load, and a tension under the pavement. For this reason, one of the issues that should be considered in the designs is the tensile deformation at the base of the pavement layer and the vertical pressure deformation on the subgrade layer [2].

There are numerous studies in the literature in which deformations occurring in road structures subjected to cyclic loading are investigated using the finite element method [3–8].

Permanent deformations accumulated due to repetitive traffic loads cause structural deterioration and constitute a significant part of the total ground settlements [9]. However, it is stated that the stresses caused by the loads on the road surface and the size of the loading cycle decrease with the depth as they spread to the ground, and the opposite situation prevails near the surface [10]. However, Deng and Shi [11] stated that rutting and permanent deformation occurring in the pavement layer exist in both the surface and the sublayers. As a result, cyclic loading manifests as permanent deformation between road layers or on the road surface in the form of fatigue cracks or ruts. Deformations, especially in the type of settlement, lead to economic losses as well as

Corresponding Author: Mürüvet Özsoy Received on 03/10/2025 Accepted on 03/03/2026

DOI: https://doi.org/10.1590/1517-7076-RMAT-2025-0844

(cc) BY

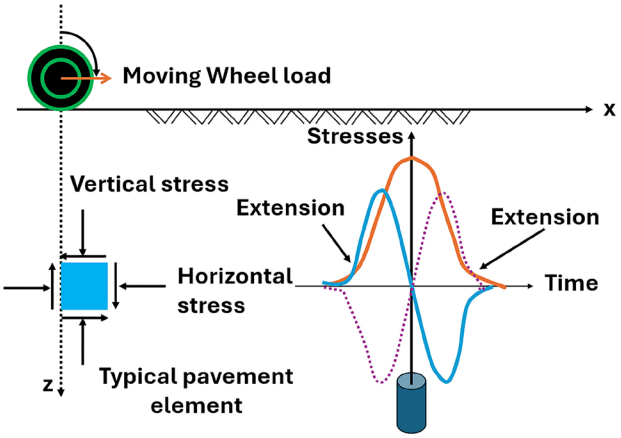


Figure 1: Stress changes under tire load [2].

serious security problems [12, 13]. Beyond negatively impacting driving safety, these damages cause the service life of the pavement to decrease significantly [7].

The deterioration in the structure of the road is also affected by variables such as the quality of the materials, the manufacturing method of the design, the loads to which it is exposed, and environmental factors [14]. The performance of materials used in road designs with complex and heterogeneous structures depends on mechanical properties and environmental conditions, as well as mixture composition and proportions [13].

Therefore, the critical design parameters of the materials used in the different layers of the road must be suitable for the general behavior and properties of the materials. It is important to consider these factors in order to determine the deterioration of the road, especially the maintenance and repair requirements [15].

There are difficulties in accessing quality raw materials due to the spread of urbanization and the increase in the use of limited natural resources. Thus, in this study, steel slags, which are formed as a by-product steel production, were preferred instead of natural aggregate. Steel slag constitutes approximately 15–20% of the amount of steel production, being the solid waste generated during the steel production phase [16]. In another study [17], it is reported that steel slag is generated in substantial amounts globally, representing nearly 20% of the world's total solid waste.

Steel slag is preferred as a durable aggregate due to its resistance to shear and abrasion [18]. According to the numerical analysis results of the studies that preferred steel slag over natural aggregates, steel slag was found to have a positive contribution to performance [19–22].

In a study conducted to evaluate the environmental contributions of steel slag, it is stated that the addition of steel slag to the stone mastic asphalt (SMA) mixture reduces greenhouse gas emissions by 1.1%–8.6%. At the same time, 14.4% to 19.8% of the cost of steel slag mixed SMA was saved. However, it is stated that engineering performance such as fatigue, deformation, and crack resistance is superior [23].

It is also important for the future of our world to choose renewable energy sources with the use of recycled, by-products or waste materials based on environmentalist approach. Recently, the scientific community focused especially on the life cycle assessment (LCA) of selected materials in highway designs and their contribution to environmental performance [24]. In addition, innovative and sustainable designs that require less maintenance and repair are among the goals of many countries' economies [25].

In this study the effect of using steel slag aggregates to efficiently use natural resources and reduce deformations on highways, thus promoting the use of waste products, was evaluated using 3D finite element software to ensure a sustainable life cycle. Positive results were obtained in sections where was used steel slag in the base and subbase layers, compared to sections where natural aggregate was used. The contribution of steel slag usage to plastic strains was also determined. The common goal of these studies is to make environmentally friendly and sustainable designs.

2. MATERIALS AND METHODS

The aggregates in the materials used in the layers of the road are obtained as a result of the decomposition of various rocks. As a result of this separation, the products obtained as crushed stone must have chemical, physical, and mechanical properties in accordance with the specifications. In addition, the stress-strain behavior of the materials used in the superstructure affects the life and performance of the design in the long term.

As a result of the complex structure of roads consisting of many layers, perfect mathematical models are difficult to develop. Thanks to material constitutive models, the mathematical expression for the mechanical behavior of materials is possible.

It is stated that granular soils show elasto-plastic deformation in all stress states [26]. Accordingly, while soil materials behave elastically at very small unit deformation values, their behavior evolves towards plasticity in cyclic dynamic loading. Therefore, Hardening Soil with small strain stiffness (HSsmall) material, which represents elasto-plastic behavior, was chosen as the constitutive model [27].

Asphalt material is considered a visco-elastic material because of its modulus of elasticity and some deformation properties that can vary with temperature [28]. In numerical models, the Mohr-Coulomb (MC) material model, which is characterized by asphalt concrete (AC) elasto-plastic behavior, was chosen. In the base, subbase, and subgrade layers, the HSsmall material model was used, which reflects the elasto-plastic behavior as in the pavement layer.

The material properties assigned to the materials that make up the road layers are summarized in Table 1.

2.1. Steel slag

There are three types of steel slag, which is the by-product produced during steelmaking: the basic oxygen furnace (BOF) slag, electric arc furnace (EAF) slag, and ladle furnace (LF) slag [30].

According to the World Steel Association 2023 reports, global crude steel production was calculated as 1,892 million tons (Mt) an increase of 2 Mt compared to the previous year [31]. The world map given in Figure 2 shows the top 10 countries in crude steel production and their production amounts.

Table 1: Input parameters for numerical simulations in software [29].

	MATERIALS					
	BASE		SUBBASE		SUBGRADE	
	SLAG	CRUSHED STONE	SLAG	CRUSHED STONE	CLAY	ASPHALT
Modulus of Elasticity (MPa)	–	–	–	–	–	4500
ν (Poisson's ratio)	0.35	0.35	0.35	0.35	0.2	0.3
γ (kN/m^3)	23.11	21.33	22.47	20.77	18	24
c (kN/m^2)	47	40	45	40	100	525
ϕ	47	40	45	35	10	27
E_{50}^{ref} (MPa)	160	165	124	115	24	–
G_0^{ref} (MPa)	180	185	138	128	55	–

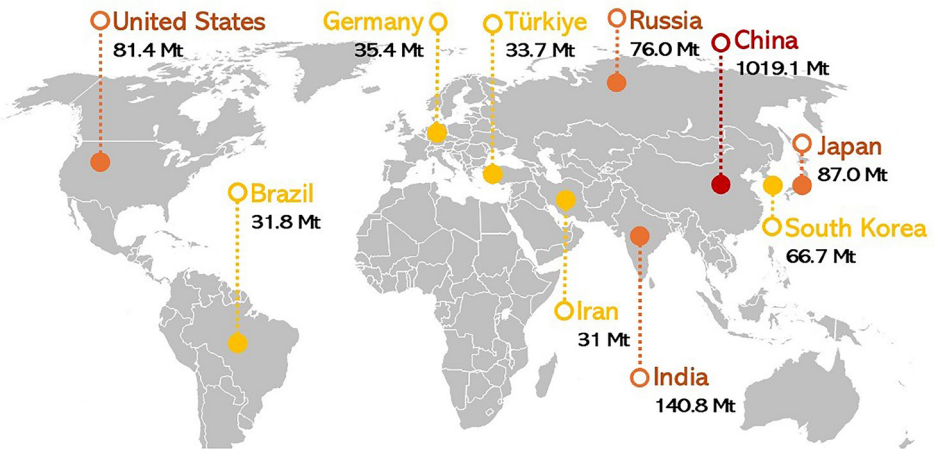


Figure 2: Crude steel production amounts of the top producing countries in 2023 [31].

The distribution of steel, which is used both as a main product, and by-product in many areas of the world, is given in Figure 3. The increase in the amount of steel slag is inevitable due to widespread and high production amounts of steel.

Steel slags were previously considered a waste product and disposed of by burying them in solid waste areas (landfills). However, in the long term, it has been involved in the recycling process to mitigate its negative effects on both the environment and human health. It is also stated that slags constitute one-third of the steel mass produced. They are seen as dangerous due to causing environmental problems, the need for large areas during the processing and storage of steel slag [32].

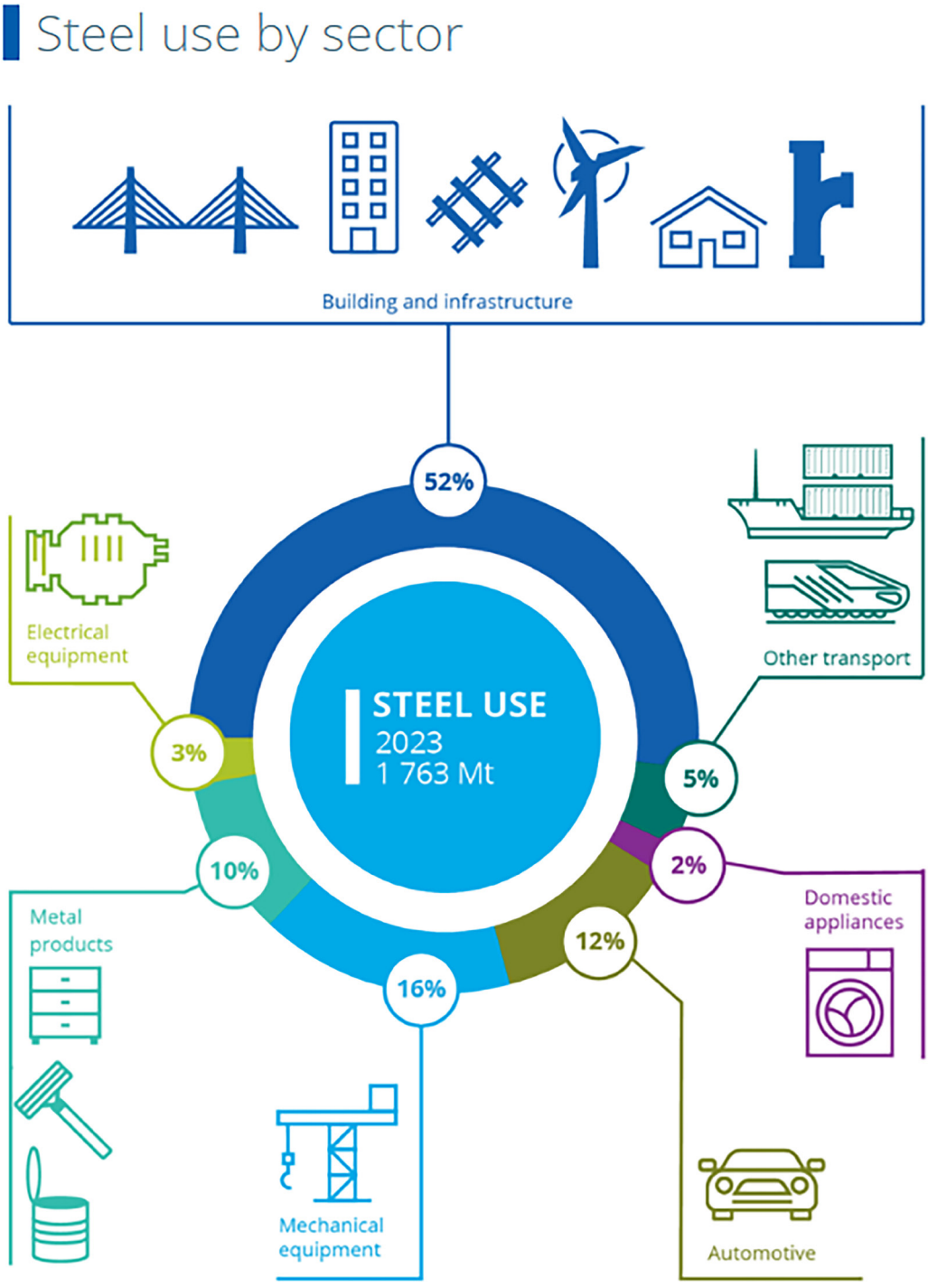


Figure 3: Areas of use of steel [31].

(cc) BY

In recent years, the slag material has been successfully used as an aggregate in both cement and concrete production plants [33–36]. Thanks to the mechanical and physical properties of steel slag, it has taken its place as a material in the high-quality aggregate class. This makes it an alternative to natural aggregate [37–41].

It is reported in the literature that the primary components of steel slag are calcium oxide (CaO), silicon dioxide (SiO_2), iron oxide (Fe_2O_3), aluminum oxide (Al_2O_3), and magnesium oxide (MgO), while MnO, P_2O_5, and TiO_2 are present in trace amounts. The chemical composition of steel slag exhibits substantial variability contingent upon the production process, furnace configuration, and feedstock, typically featuring CaO and SiO_2 concentrations of 20–55% and 10–24%, respectively [42].

Despite the potential advantages of steel slag in soil stabilization, it also possesses disadvantages such as low water-holding capacity and susceptibility to segregation [43]. A comprehensive study in the literature expressed that the long-term use of steel slag may lead to soil hardening and environmental risks stemming from heavy metals. To mitigate these adverse effects, it has been suggested to pre-treat the steel slag and combine it with other products by reducing its density in the mixture [42]. Steel slag is essentially composed of SiO_2, Al_2O_3, Fe_2O_3, MgO, and f-CaO, along with various iron-containing minerals [44]. However, the complex mineralogical composition of steel slag, particularly the free calcium oxide (f-CaO) content, poses a significant risk in terms of volumetric stability [45, 46]. Moreover, researchers [47] have indicated that the hydration of MgO and CaO constituents triggers swelling, which subsequently causes damage by compromising the cohesion and adhesive characteristics of the material.

Aggregate hardness and sensitivity to moisture damage are increased by the presence of silica and specific oxides like Fe_2O_3, MgO, and Al_2O_3 in their mineralogical structure. However, it is emphasized that the primary factor in the failure of adhesion occurring in the presence of moisture is whether moisture reaches the aggregate–bitumen interface or not. In this context, it has been reported that even if the aggregates used in steel slag mixtures have the potential for moisture damage, when aggregates are completely and continuously coated with bitumen, moisture is prevented from reaching the interface. Consequently, it has been reported that adhesion degradation is significantly reduced [48]. The same study also expressed that the absence of clay and organic contaminants on the surface of slag aggregates is instrumental in their lower potential for moisture damage compared to other aggregate types.

Additionally, it is stated that some types of untreated steel slag exhibit low adsorption efficiency due to their low surface activity [49]. In contrast, due to its absorption of heavy metal ions, steel slag stands out as a potential treatment material for the purification of various wastewaters [50, 51].

Considering the preservation of natural resources, the reduction of environmental impacts, and the versatile technical advantages it provides, the use of steel slag in road construction is of great importance and is regarded as a critical necessity for sustainable infrastructure applications.

The World Steel Association reported that approximately 38.5 million tons of steel slag was produced in the European steel industries in 2022, depending on the amount of crude steel produced. These products participate in the recycling process in road construction (64.8%), metallurgical use (12.1%), cement/concrete additive use (6.9%), fertilizer (8.1%), hydraulic engineering (1.9%), and other application areas (6.2%) [52].

On highways, if steel slag is preferred as an aggregate in the asphalt layer, slag increases the strength of bituminous mixtures and slows down cracking due to better asphalt-slag adhesion [53]. Furthermore, it has been indicated that the high angularity and surface roughness of steel slag aggregates facilitate greater tire-pavement friction, thus playing a significant role in enhancing skid resistance. [54]. In a field study [55], it was demonstrated that the pavement layer prepared using EAF slag provided better performance in terms of stiffness, fatigue, and permanent deformation compared to conventional hot mixes.

From an environmental perspective, ensuring the inclusion of waste materials in recycling activities is among the popular methods today in terms of sustainability.

It is necessary to consider the use of sustainable materials such as steel slag within acceptable limits and also their possible disadvantages. However, there are points to be considered when using steel slag. In addition, the reason why steel slag shows superior properties is that it is preferable in terms of mechanical properties as a very dense, hard, and high-strength material. Reusing it in construction applications for recycling purposes will be a sustainable and cost-effective alternative to waste management.

2.2. Physical and geotechnical properties of steel slag

Table 2 gives the geotechnical properties of steel slag used in numerical analysis. Parametric studies based on the literature were also carried out to determine the qualities of the steel slag to be used in road layers as aggregate. The specific gravity value of steel slag was calculated as 2.9 from the experimental study.

(cc) BY

Table 2: Geotechnical properties of steel slag.

GEOTECHNICAL PROPERTIES OF THE SAMPLES	
PROPERTIES	**SUBBASE/BASE**
USCS	SP
Gravel (%) (D>4.76 mm)	33.2
Sand (%) (0.074 mm<D<4.76 mm)	64.2
Fines Content (%) (0.074 mm)	2.6
Cc	0.69
Cu	9.49
$\phi(^{\circ})$	45/47
c (kPa)	45/47
$\gamma_{d\ max-\ standart}$ (kN/m^3)	1.66
$w_{opt-\ standart}$ (%)	20.39

2.3. Creation of road model using finite elements method

Numerical methods are an important tool preferred in the analysis of problems in research and application studies, especially in geotechnical engineering, as well as in many engineering disciplines [56]. In particular, the finite element method (FEM) is one of the most preferred numerical methods. FEM is a numerical method that offers an estimated solution approach for each element after dividing a single element into a large number of elements [57].

Numerical models created with FEM have the advantage of evaluating different parameter effects at low cost [58]. It is also ensured that a numerical solution approach is designed to accurately address many engineering problems using FEM.

3D modelling provides greater consistency between the value estimated by the numerical analysis method and the measured value compared to the 2D model [59]. In addition, 3D models can define model geometries with more accurate loading configurations compared to 2D axisymmetric models in representing behavior under cyclic loads [60].

In multi-layered road designs, numerical methods are preferred to measure the mechanical reactions that can occur due to vehicle traffic and environmental factors [57, 61, 62]. Significant developments in computer technology and FEM techniques in the last thirty years have made many widely used 3D structural studies more affordable when evaluated in terms of both time and cost. In addition, 3D FEM is widely preferred so that the tire-retread interaction can be fully reflected, and the design can be simulated more realistically [62, 63].

There is many software that uses the finite element method such as, which have been widely preferred recently, Plaxis, ABAQUS, ANYS, ILLI-PAVE, KENLAYER, CHEVRON, VESYS, FENLAP, MICH-PAVE and Midas GTS NX, to accurately calculate nonlinear material behavior in road design. The type of software selected varies depending on the factors such as material behavior, design and calculation type of the model to be numerically analysed. Midas GTS NX is a finite element analysis software developed for the analysis of soil-structure interaction or soil structures only in 2D and 3D. In addition to the presence of constitutive models in the software library that allow modelling of a large number of materials, the dynamic and static analysis, linear/non-linear time analysis, and the definition of different boundary conditions are possible [29].

In addition to the creation of numerical simulation models, quickly accessing outputs, as well as addressing the stress limits from analyses, are issues to consider in selecting model dimensions. It is preferable the geometry of the FE model to be created with optimum dimensions that do not contradict reality, in order to reach the fastest result while establishing and analysing the model numerically.

The superstructure model consists of four layers: pavement, base, subbase and subgrade layers. Finally, numerical analyses were performed for four different road sections Limestone-Steel Slag (LS), Steel Slag-Steel Slag (SS), Steel Slag-Limestone (SL), and Limestone-Limestone (LL) in which steel slag and natural aggregates were used in the base or subbase layers. The asphalt concrete layer (AC) refers to the pavement layer. In order not to cause discontinuities in the analysis, it is important that it is of sufficient size and should a size that reflects the field conditions.

(cc) BY

Figure 4 shows the cross-sectional layer thicknesses of four different roads. The thickness of the layer is modelled at 100 mm for pavement, 300 mm for the base layer, 400 mm for the subbase layer, and 5000 mm for the subgrade layers, respectively. The longitudinal and transverse lengths of the 3D road model were determined as 30 m and 8 m.

The size and arrangement of elements in a mesh can have a critical impact on the accuracy of an FE analysis. A poorly formed mesh is a common source of error, so significant attention should be given to mesh quality, and automated mesh generators cannot be relied upon to produce good mesh [64]. The numerically analysed model is depicted in Figure 5.

The calculation time in numerical analysis increases the density of the mesh system and the complexity of the model. The need for additional storage capacity and time in simulations using 3D FEM software has been expressed in many studies [28, 65]. Mesh dimensions affect the precision and duration of numerical analysis. Correct dimensioning is one of the most crucial elements that enables simulations to be calculated as close to reality as possible. For this reason, a mesh system should be created starting from small areas and the regions where load concentrations accumulate should also be considered in the selection of mesh sizes. In line with these statements, mesh elements with smaller dimensions were used in the wheel loading areas and the element sizes were increased in the layers moving away from the loading area. In this way, the goal is to reach the most accurate result in the optimal time.

The size of the mesh system that is used the 3D FEM model and the accuracy of the calculations are based on the sensitivity analysis [29]. In the sensitivity analysis, the aim is to avoid convergence errors and to determine the optimal mesh sizes without causing problems in calculation time and storage capacity. While the mesh element sizes in the loading area are smaller, the element sizes are increased as they move away from the loading area.

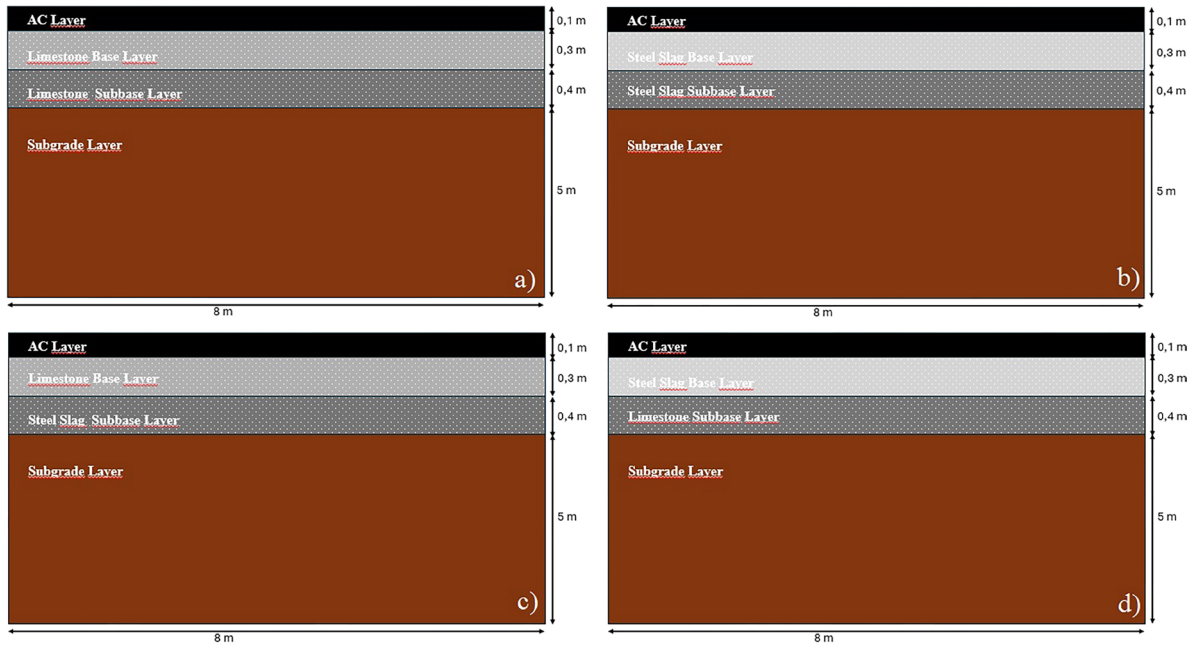


Figure 4: Cross sections of road layers a) LL, b) SS, c) LS, d) SL.

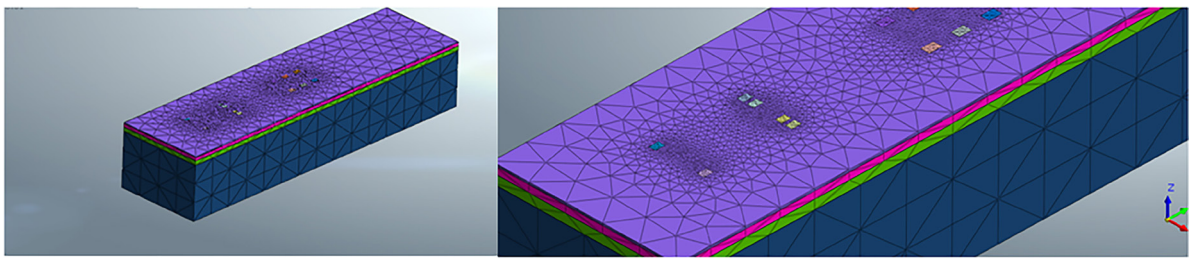


Figure 5: FE model with numerical analysis.

This model has 4216 nodes and a total of 16905 elements. To maintain continuity in the model, the shapes and sizes of the layers are kept the same both horizontally and vertically.

2.4. Definition and geometrical properties of loading areas

Some studies have been carried out to determine the contact behavior between the tire and the pavement layer [66–70]. The main objective of the studies is to evaluate the basis of tire-retread contact behavior; it is of immense importance in terms of improving the performance of the road, increasing the service life, and energy saving [71].

According to PIDWERBESKY [72], increases in axle load and tire pressure have a major impact on retread response. The effects of vehicles on the asphalt surface are realized by the contact of tires.

Depending on the contact shape and area, there are geometric properties of the tire pavement interaction. In addition, the geometric shape of the tire-pavement contact area is circular or rectangular and is based on the assumption that it has uniform pressure distribution. At the same time, many studies have been carried out on the geometric properties of the tire-pavement contact [73–76]. These simplified approaches are widely used in pavement design [77].

There are many studies that evaluate the effect of tire inflation pressure and tire load on the contact area [78–80]. It has been determined that with the increase in tire pressure, the contact area decreases. This increase in tire pressure also elevates the contact stress in the middle of the wheel. While, meanwhile, the stresses on the tire edges increase if the tire load increases [81].

The tire-pavement contact area is usually assumed to be circular or rectangular and to have uniform pressure distribution [69]. The simplified model of HUANG [82] for modelling the contact field between the tyre and the retread is preferred. The image of this model is given in Figure 6.

Field measurements were made to determine the tire contact areas on the front and rear axles of the heavy vehicle. By measuring the tire widths in the front axle, tandem, and tridem zones of the loaded heavy vehicle, the other dimension of the tire loading area was determined using Huang's simplified contact field equation (Figure 6). In Figure 7, the loading area and wheel dimensions of the heavy vehicle are given.

The tire sizes calculated as a result of the measurement in the wheel loading areas, they are modelled as 3D solid elements in the software, as shown in Figure 8.

3. RESULTS

The deformations caused by heavy vehicles, which are widely preferred in freight transportation all over the world, are much higher than those caused by other vehicles. Heavy vehicles cause more damage to road structures. Therefore, the Annual Average Daily Traffic (AADT) and the percentage of heavy vehicles are the main factors affecting the axle load of the road section, traffic accidents and possible pavement distress [84].

Considering the inflation pressure of 100–110 psi of the heavy vehicle in the tire loading areas modelled in Figure 9, the wheel contact pressure that 700 kPa was enforced using triangular loading distribution. The tire contact pressure is evenly distributed over the rectangular area.

For simplification, it is assumed that the contact stress of each tire is a constant pressure evenly distributed over the contact area [83].

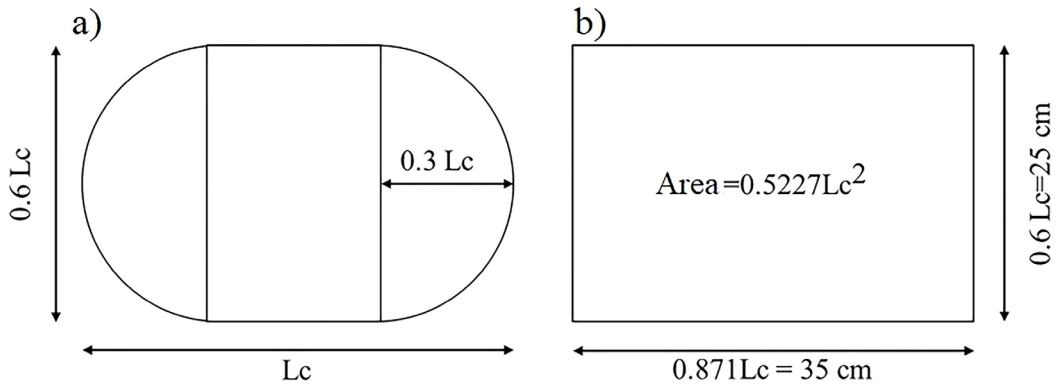


Figure 6: Simplified tyre contact area calculation: a) Actual contact area (b) Equivalent rectangular contact area [82].

(cc) BY

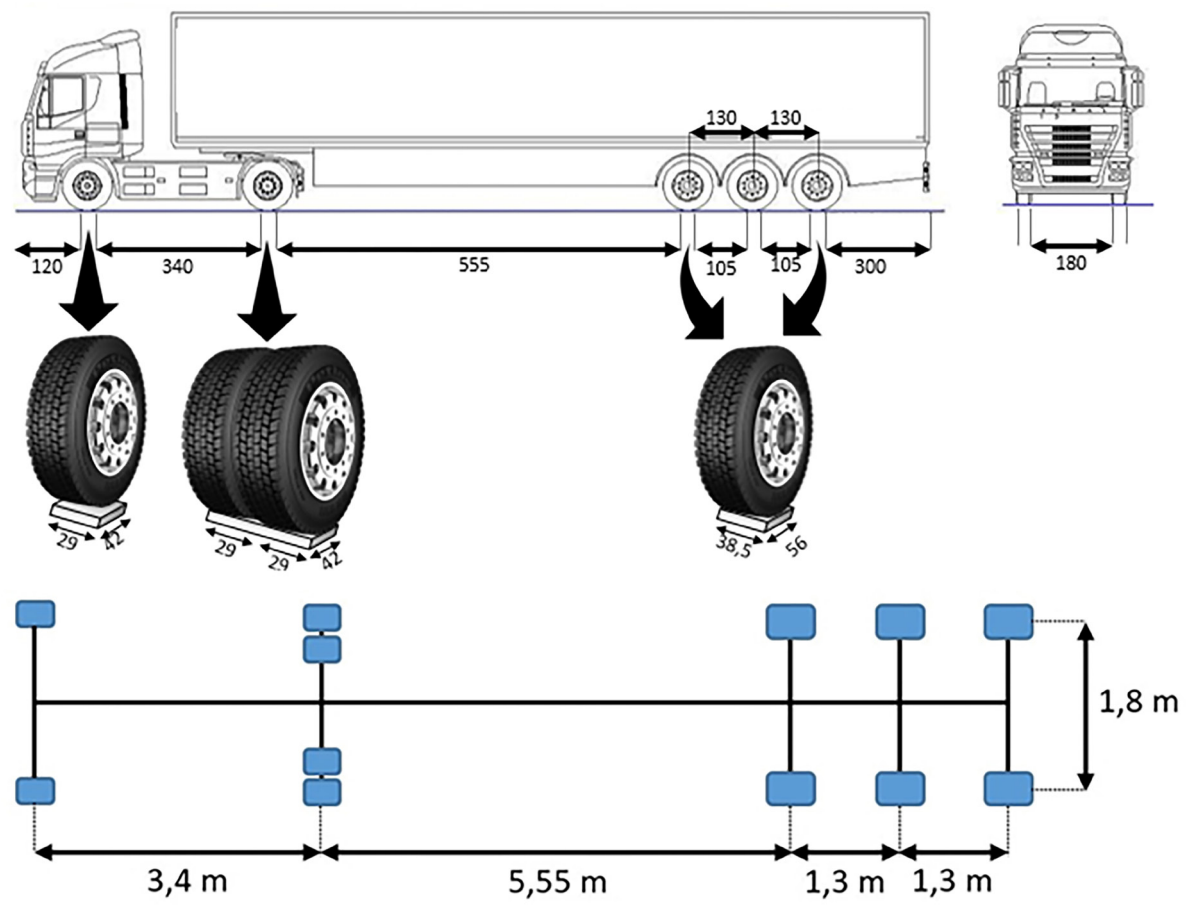


Figure 7: Schematic representation of heavy vehicle wheel loading area dimensions used in numerical model [83].

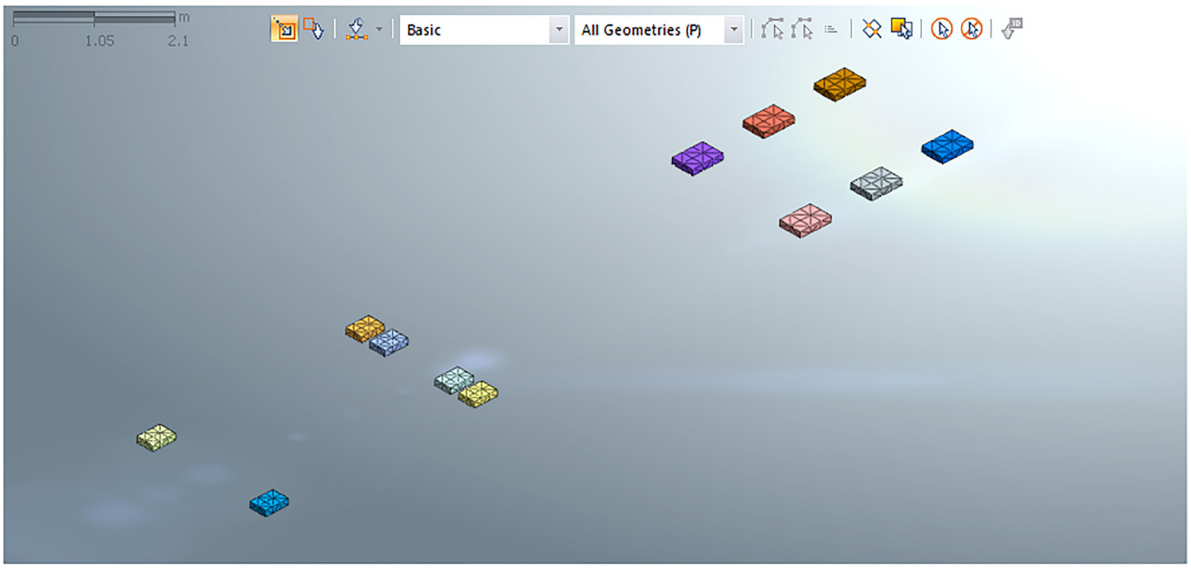


Figure 8: 3D wheel loading areas.

In addition, the impact duration of the applied wheel load is one of the important calculation parameters that must be determined to perform dynamic analysis. For this purpose, in determining the impact duration, HUANG [82] proposed Equation 1, which depends on the speed of the vehicle and the tire contact radius. d is the duration of the pressure pulse, s is the value of the vehicle's speed in m/s, and a is the tire contact radius. The application time of the wheel loading pressure was calculated as 0.139 seconds.

(cc) BY

$$d = 12 * \frac{a}{s} \tag{1}$$

There are studies in which sinusoidal [85], semi-sinusoidal [28, 85], trapezoidal [86] and triangular [87] distributions of loading pulses are used. Considering both storage space and calculation time, the contact stress was applied in the form of a triangular loading pulse, as shown in Figure 9, because using this form requires fewer sub-steps compared to other loading types.

After ensuring that the contact surfaces between the layers are loaded, a finite element mesh is created and the materials defined by the user are assigned to each layer. After determining the superstructure parameters, geometry and vehicle tire configuration, numerical analysis is performed.

3.1. Nonlinear time history

In general, most soil materials have non-linear properties. Therefore, the dynamic response of the soil can be accurately simulated using nonlinear time domain analysis. Nonlinear time-domain analysis is used to determine the dynamic response in a relatively short period of time.

Elasto-plastic deformations occur in some soil types under the influence of dynamic loading. While plastic deformations continue to increase cumulatively with each loading cycle, elastic deformations are reversible. For this purpose, the use of viscous damping parameters is important because elastic behavior does not affect subsequent dynamic load steps. Due to the large number of degrees of freedom of the 3D FE model, the damping parameters are defined by a matrix form in which the coefficient C is calculated based on the Rayleigh damping approximation considering the system mass and rigidity. The equation for the coefficient C is given in Eq. 2. The mass and stiffness parameters of the system are M, and K depend on the vibration frequency and damping rate. α and β are the Rayleigh coefficients. It depends on the vibration frequency and damping ratio.

$$C = \alpha M + \beta K \tag{2}$$

However, within the scope of the numerical analysis, the vibration periods of the modes with high mass participation rates were calculated by Eigenvalue analysis. The damping parameters of the model system are defined.

In stepwise analysis, which is defined as stress and time-dependent, the model is primarily analysed under its own weight. Afterwards, nonlinear time analysis is performed.

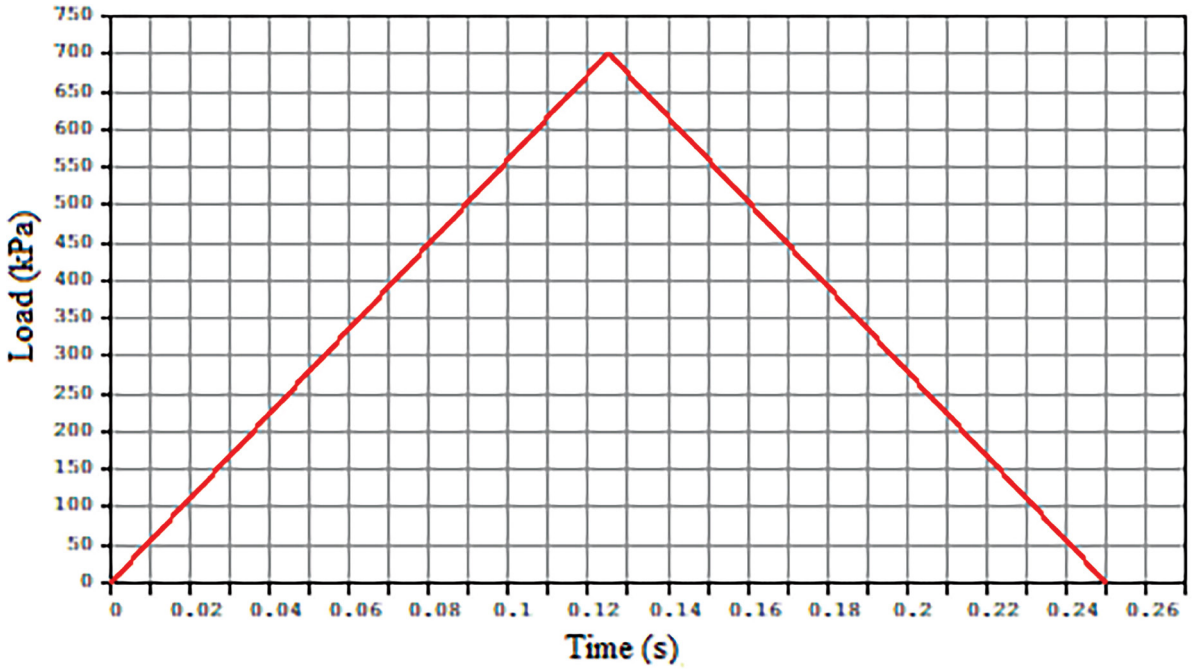


Figure 9: Dynamic upload form shape.

(cc) BY

In the numerically analysed mathematical model, the model edges are only allowed to move in the vertical direction (see Figure 10 for the boundary conditions). The movement of the layers in the horizontal direction is restricted. On the basis of the model movement in all directions is not allowed.

In the numerical analysis, the vertical settlement value created by the dynamic vehicle load in the pavement layer is considered.

3.2. Evaluation of the impact of steel slag use

For sections with different base and subbase material compositions (LL, SL, SS and LS), the vertical deformation of the asphalt is evaluated. The stress generated as a result of dynamic loading is distributed between the layers in systems with layered designs and transmitted to the natural ground. For this reason, the deformation value on the asphalt surface is considered. The contour distribution in the model as a result of the calculations defining the loading steps in Figure 11.

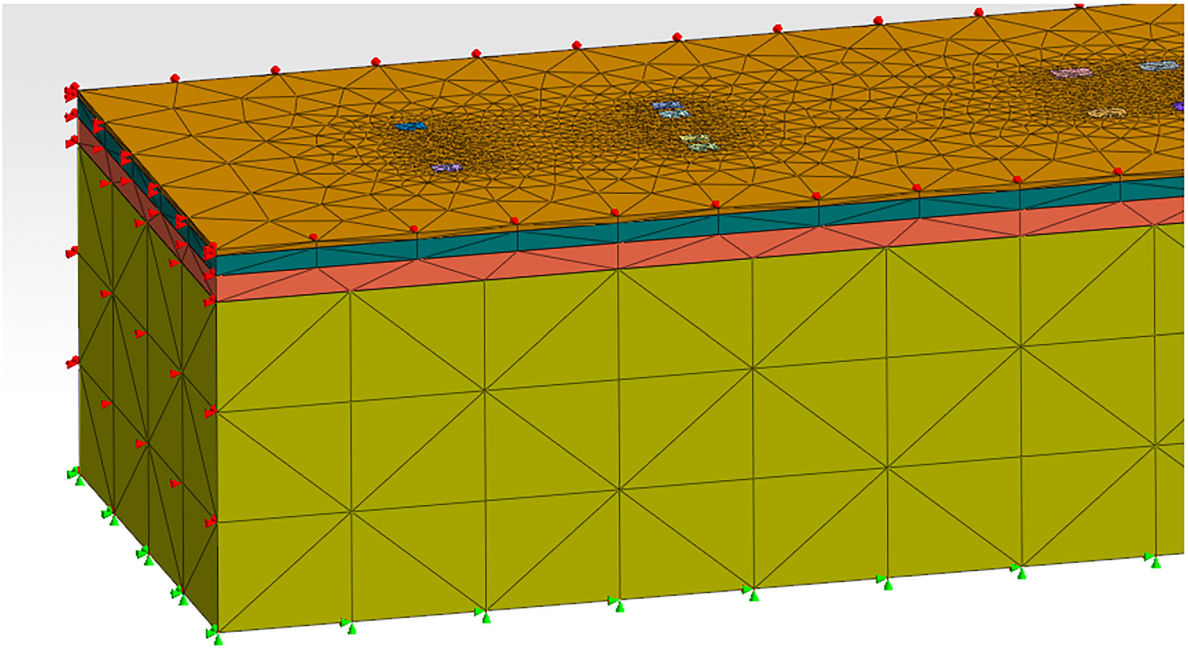


Figure 10: 3D model boundary conditions.

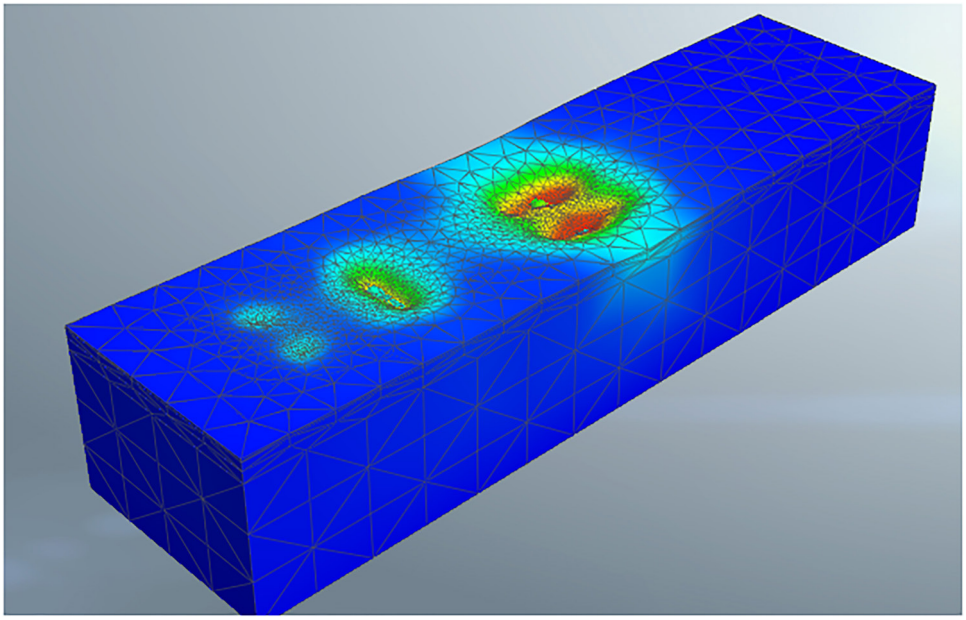


Figure 11: LS section deformation image.

(cc) BY

The highest deformation value was determined in the truck bed part of the heavy vehicle as a result of numerical analysis.

Time-dependent vertical deformation change values are observed at the reference points determined in Figure 12 along the middle axis of the tridem region.

Based on the deformation pattern in the LS section given in Figure 11, time-dependent vertical deformation change values are observed at the reference points determined in Figure 12 along the middle axis of the tridem region.

The typical time-dependent change curves for SL sections of the vertical deformation value that occur as a result of the response of the pavement layer to dynamic loads as a result of repeated loading cycles are given in Figure 13. In this figure, the axial deformation behavior of the sections using steel slag and natural aggregate taken from the reference points is shown. Deformation-time graphs for other sections are given in Figures 14, 15 and 16.

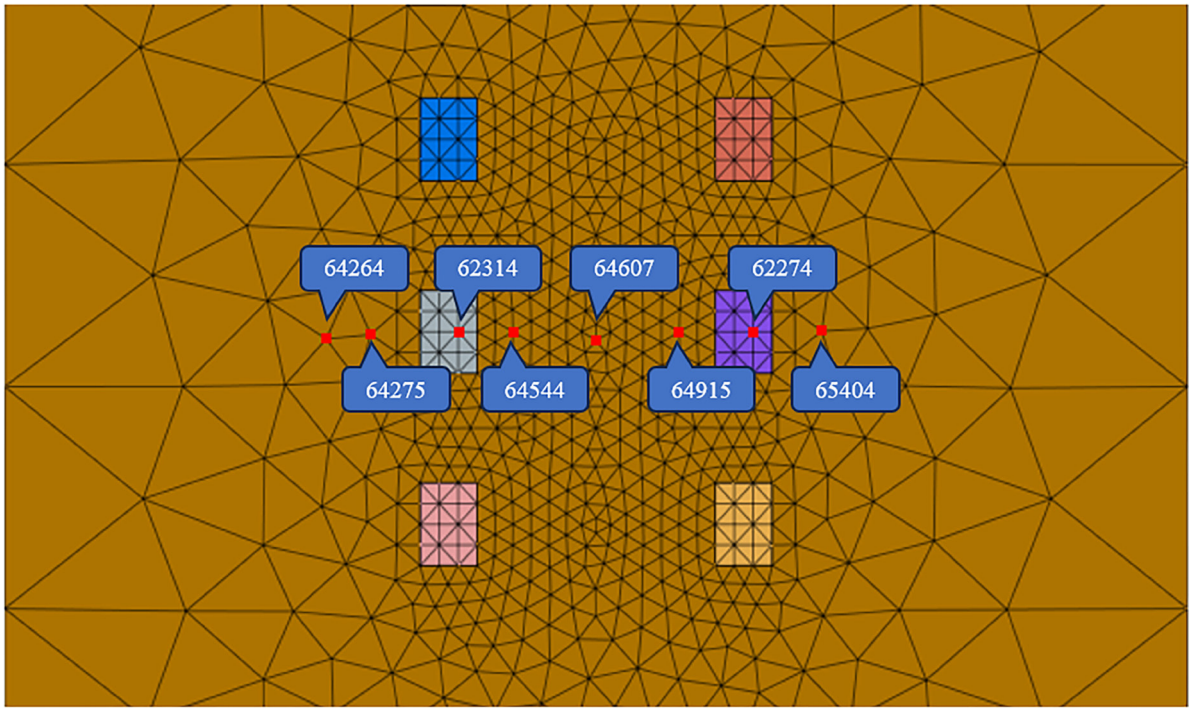


Figure 12: Vertical deformation values reference points in 3D model [29].

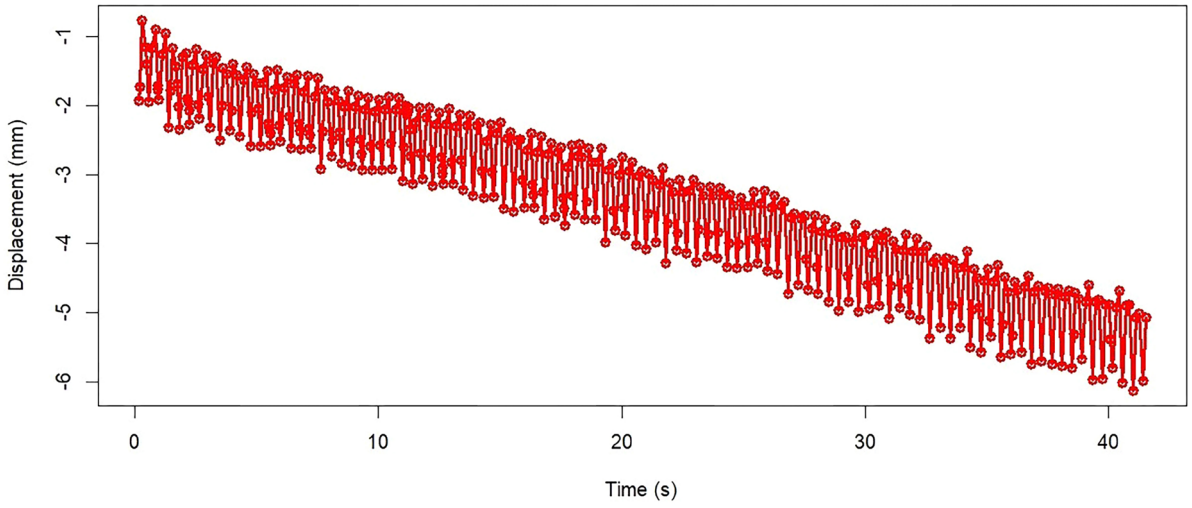


Figure 13: SL cross-section, N = 100, loading step, vertical deformation-time change curve.

(cc) BY

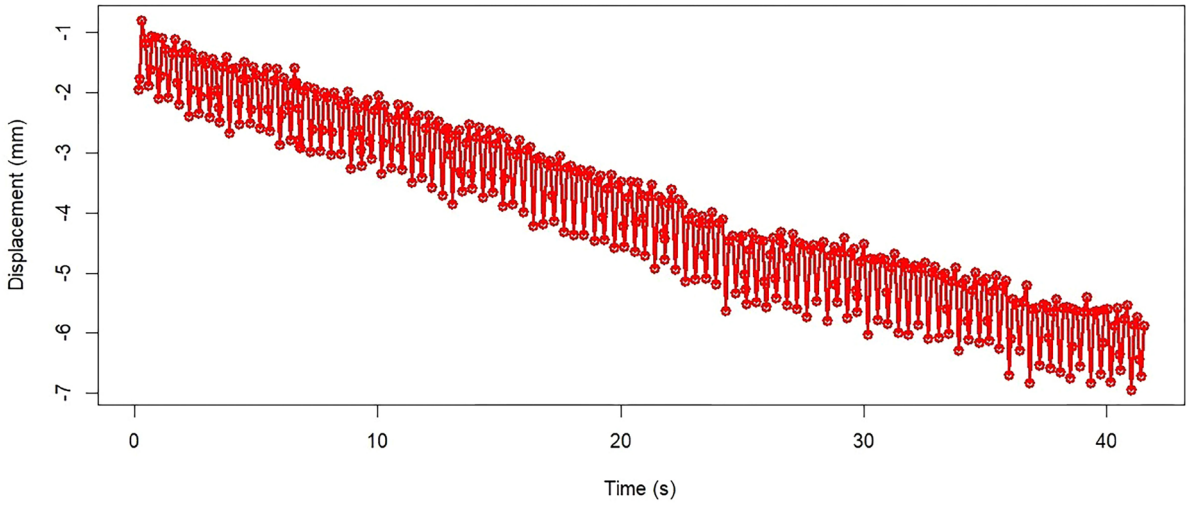


Figure 14: LL cross-section, N = 100, loading step, vertical deformation-time change curve.

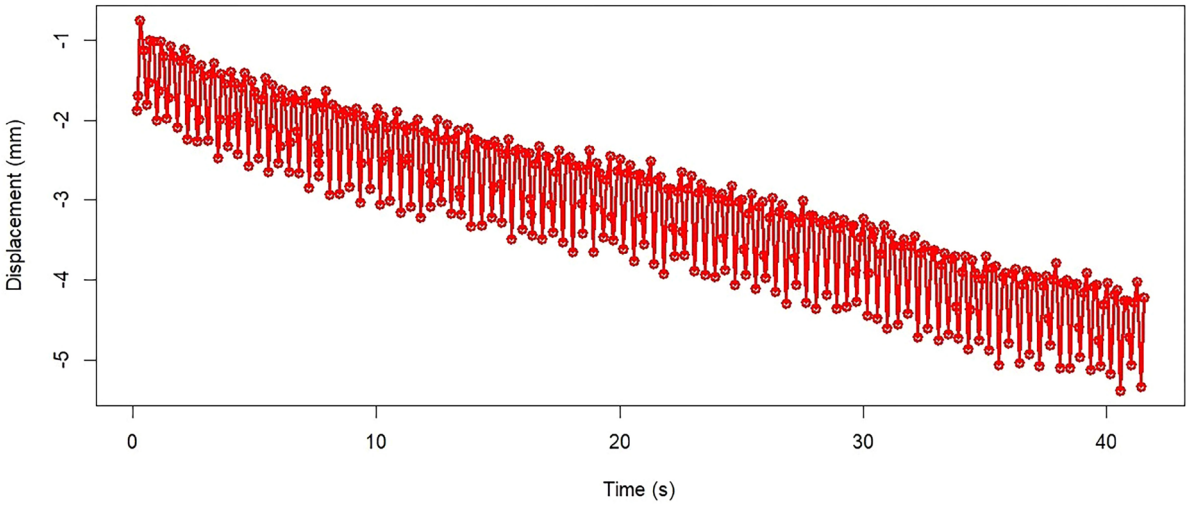


Figure 15: LS cross-section, N = 100, loading step, vertical deformation-time change curve.

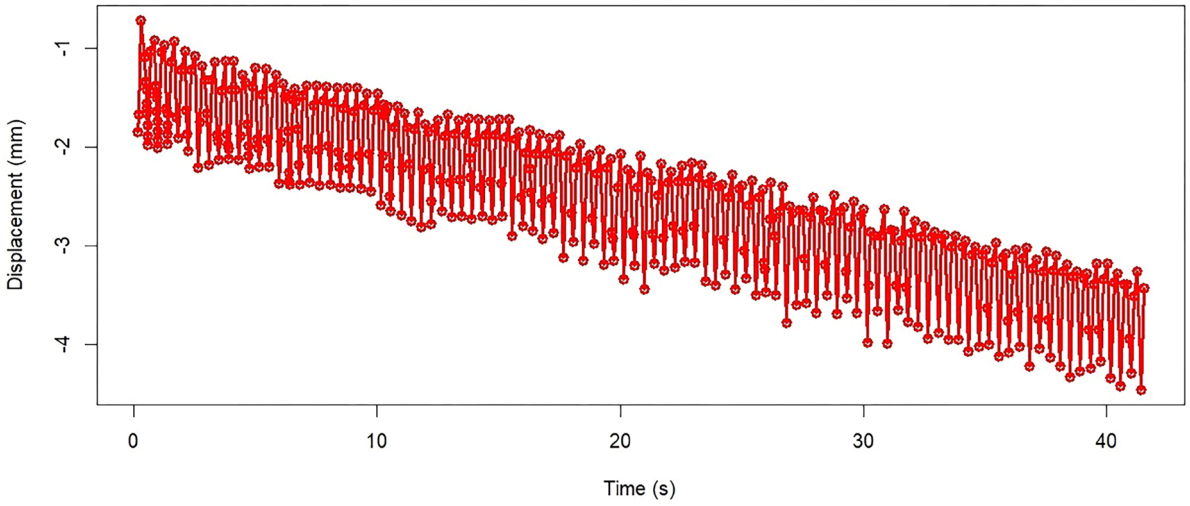


Figure 16: SS cross-section, N = 100, loading step, vertical deformation-time change curve.

(cc) BY

In the dynamic analysis based on the triangular shaped loading of 700 kPa, vertical deformation values were primarily taken into account when used in the base and subbase layers of steel slag. The minimum vertical deformation value in the model sections with a maximum of 100 loading steps was calculated as 4.47 mm in the SS section. This value is up to 6.95 mm in the LL section. The curve of change in the settlement values depending on the loading steps of the sections is given in Figure 17.

The deformation values in the first 10 loading steps are very close to each other. Numerical differences between sections have also started to emerge with the increase in the number of uploads. Within the range of 10 to 100 loading steps, the most vertical deformation occurred in the LL section where natural aggregate was used in the base and subbase layers. After the N = 15 loading step, the lowest deformation is obtained in the SS section.

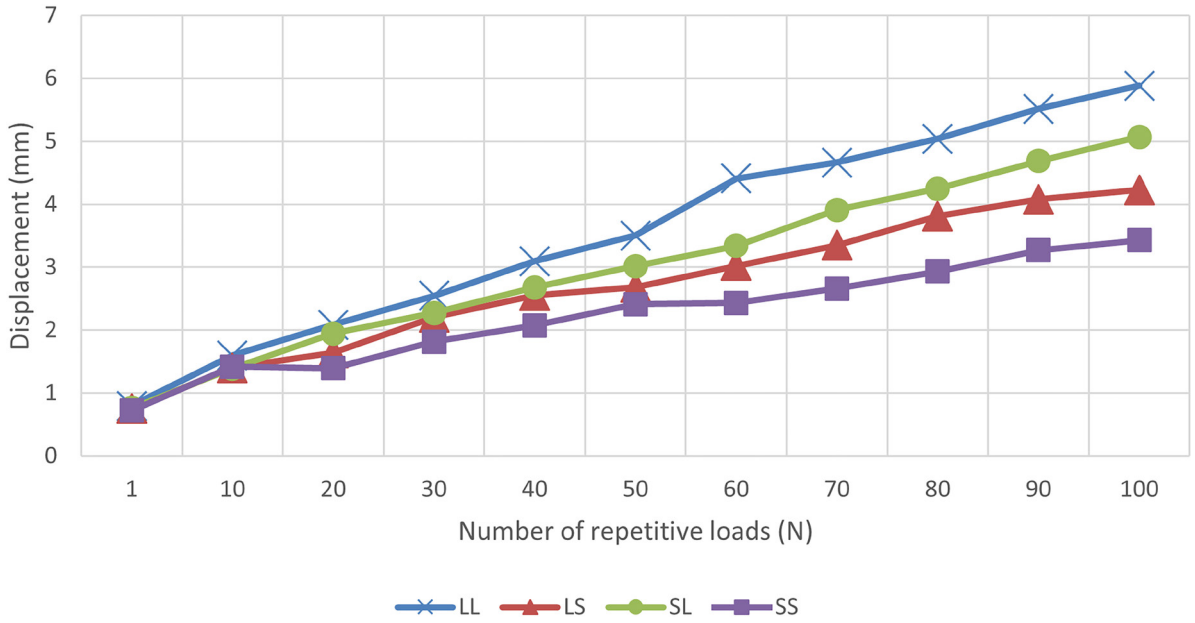


Figure 17: Loading step of sections - seating curve change.

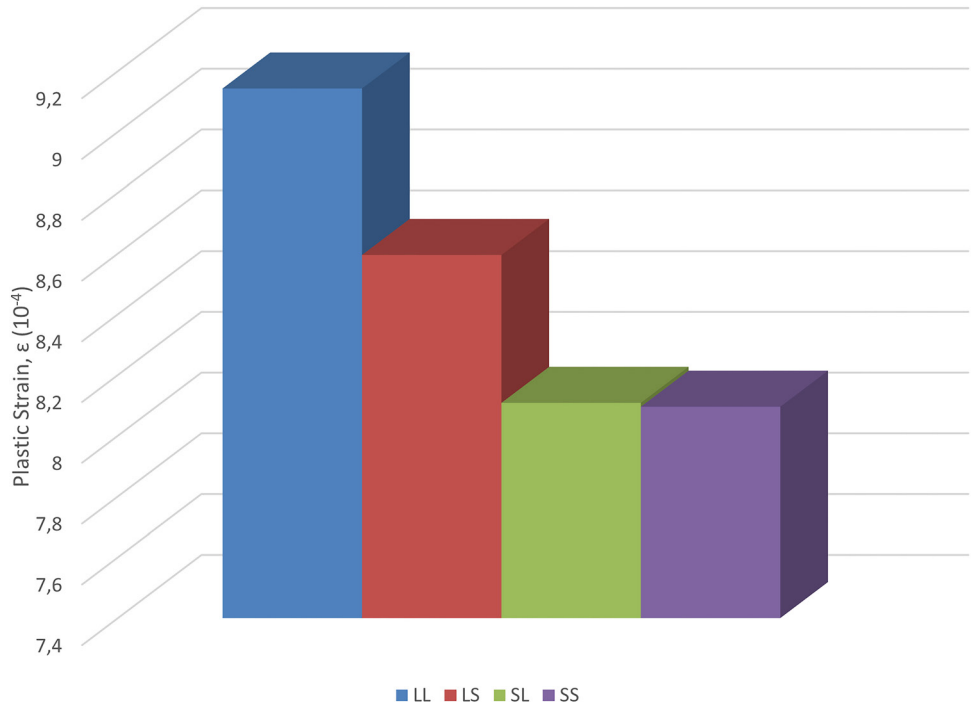


Figure 18: Plastic deformation value on natural ground.

The effect of steel slag use on plastic deformations on the natural ground (Figure 18) is evaluated as a result of the transfer of dynamic loads from the superstructure to the natural ground through the layers. The most plastic deformation occurred in the section where natural aggregate was used in the base and subbase layers. There is a difference of about 15% between the highest and the lowest plastic deformation.

As a result of the numerical analysis, when the stress values occurring in each layer are controlled, the stress distribution values in the subbase and natural soil layers are lower compared to the other layers. This indicates that the stress distributions decrease as they move away from the loaded layers. Due to the high dynamic modulus and superior engineering performance of steel slag, its positive contribution to plastic deformation on natural ground as well as vertical deformation has been proven thorough numerical analysis.

4. CONCLUSIONS AND DISCUSSION

In this study, the effect of the use of steel slag in road foundation and/or subbase layers on the vertical settlement value, particularly in comparison with natural aggregate, is evaluated. In order to represent the behavior of granular layers, the HSsmall material constitutive model is used, while elasto plastic Mohr Coulomb is used in the asphalt layer.

To investigate the vertical deformation measurements that occur due to tire-road contact, different combinations of cross-sections are analysed. The FEM is used to determine the response of the road under heavy vehicle loads.

In the multi-layer flexible superstructure system, the settlement on the surface is considered. In addition, in this system, which is built in layers, the plastic strain values that occur on the natural ground with the transfer of the dynamic wheel load applied to the asphalt layer are compared in sections with natural aggregate and steel slag.

The present research investigates and compares the deformation response of different material blends subjected to cyclic dynamic loads. These assessments were carried out specifically under dynamic loading scenarios.

- The color spectrum distributions in the deformation images are the same for the four sections examined. However, the difference between them lies in the numerical values of the deformations. It is known that the loading pressure reaches its maximum values in the wheel-tread contact areas. Accordingly, the highest deformations occurred at the tread-tire contact surface. However, it was determined that the highest levels of deformations were reached in the tridem axle region within the 12-wheel loading configuration.
- In all sections, displacement values increased with increasing load cycles. In the initial loading phase (N = 1), vertical deformation values ranged from 0.7–0.9 mm, and the difference between groups remained below 10%.
- After N = 50 loading steps, the displacement values were measured as approximately 3.4 mm, 3.0 mm, 2.8 mm, and 2.4 mm for the LL, SL, LS, and SS sections, respectively. The deformation value in the LL section was found to be approximately 42% higher compared to the SS section.
- After N = 100 load cycles, the displacement value in the LL section reached approximately 5.9 mm, while in the SS section this value was determined to be approximately 3.5 mm. At this stage, the total deformation in the LL section was approximately 69% higher than in the SS section.
- At the same load frequency level, the displacement values measured in the SL and LS sections are approximately 5.1 mm and 4.3 mm, respectively, which are approximately 46% and 23% higher, respectively, compared to the SS section.
- When comparing the deformation increase rates, it was determined that the LL section exhibited the highest increase rate throughout all load cycles, while the SS section showed the lowest and most controlled deformation behavior.
- The highest level of plastic strain was observed in the LL section relative to all other configurations. Such a finding demonstrates that the LL section possesses a higher propensity for plastic deformation during cyclic loading.
- SL and SS sections yielded the lowest and closest results, with plastic deformation values of approximately 8.2×10^{-4} and 8.3×10^{-4}, respectively.
- The overall ranking is LL > LS > SS ≈ SL, with plastic deformation in SL and SS sections reduced by approximately 10–12% compared to the LL section.
- These findings distinctly indicate that SL and SS sections offer superior performance regarding plastic deformation resistance under cyclic loading.

(cc) BY

- It is evident from the numerical analysis that the deformation response of the pavement under heavy cyclic loads is governed by the selection of material combinations.
- Considering the rates of increase of vertical deformation values between the cross-sections, it was determined that the SS cross-section is a more suitable option for pavement systems subjected to long-term repeated loading.
- The stiffness imparted by steel slag in road layers effectively mitigates vertical deformation, ensuring improved structural stability under loading.

As a result, these findings can be achieved by adding steel slag directly or to mixtures, which can provide environmental and economic advantages. At the same time, using steel slag in these ways will prevent the environmental risks that would arise from its disposal. The common goal of the studies is to make environmentally friendly and sustainable designs.

The results obtained in terms of both vertical settlement and plastic deformation indicate that the use of steel slag in base and subbase layers offers better performance compared to natural aggregates. This situation can be attributed to the high hardness, angular particle shape, and high internal friction properties of steel slag. Additionally, the strong adhesion of steel slag with asphalt contributes to increased wear and fatigue resistance of the pavement. Studies in the literature support these findings, and the positive effects of steel slag on mechanical performance have been similarly expressed in various researches [43, 88–91].

The quality of the materials used is very important to ensure that the road structure can endure a large number of repetitive traffic loads and be strong enough to resist the deformations caused by wheel loads. Relevant research [13, 92, 93] also underscores the importance of this phenomenon. In addition to the new construction techniques used, the use of materials that will contribute to recycling has been increasing in recent years. In the literature, it is observed that studies on improving performance through the use of materials with different compositions and engineering properties in road pavements are ongoing, and this approach has a decisive impact on pavement behavior [54, 94–99].

The replacement of traditional aggregates, which are widely used in the design of the layers that make up the road, with such steel slag materials is also promising for sustainability. It is possible to say that the preference of sustainable soil improvement methods [45, 55, 99–103] will become the focus of research in the future due to the decrease in limited resources.

In this study, the behavior of the pavement structure under dynamic loads was investigated using 3D FEM. While FE analysis is a reliable method for evaluating pavement-tire interaction, the assumptions, idealizations, and boundary conditions made during the modeling process affect the results. The mechanical behavior of materials is described by constitutive models commonly used in the literature; however, these models can only represent the time-dependent behaviors, temperature effects, and environmental variables that occur in field conditions to a limited extent. In this context, conducting studies supported by field measurements and experimental data in future research is considered important for model validation. Future studies are recommended to include validation studies supported by field measurements and laboratory experiments. Furthermore, incorporating environmental factors such as temperature variations, climatic conditions, and groundwater levels into numerical models will contribute to a more realistic representation of field conditions.

Another limitation of this study is that, due to experimental equipment and practical constraints, the mechanical properties of steel slag were not primarily evaluated. The chemical interactions, volumetric changes, and long-term degradation mechanisms of steel slag could not be experimentally investigated within the scope of this study; assessments in these areas were limited to existing information in the literature. Therefore, chemical reactions and time-dependent behaviors that could affect the long-term performance of steel slag were excluded from this study. Future research is recommended to utilize comprehensive experimental investigations to examine the long-term degradation behavior, infiltration potential, and chemical interactions of steel slag with the soil/pavement environment.

5. ACKNOWLEDGEMENTS

The author thanks the Editor-in-Chief, and anonymous referees for their insightful comments and suggestions.

6. BIBLIOGRAPHY

[1] EUROPEAN COMMISSION, *EU transport in figures: statistical pocketbook 2021*. 2021, https://data.europa.eu/doi/10.2832/27610, accessed in January, 2025.

(cc) BY

[2] BROWN, S.F., "Soil mechanics in pavement engineering", *Geotechnique*, v. 46, n. 3, pp. 383–426, 1996. doi: https://doi.org/10.1680/geot.1996.46.3.383.

[3] QIAN, G., SHI, C., YU, H., *et al*., "Evaluation of different modulus input on the mechanical responses of asphalt pavement based on field measurements", *Construction & Building Materials*, v. 312, pp. 125299, 2021. doi: https://doi.org/10.1016/j.conbuildmat.2021.125299.

[4] YANG, J., XIE, J., TANG, X., *et al*., "Study on the permanent deformation of asphalt mixtures based on the modified Burgers model", *Frontiers in Built Environment*, v. 10, pp. 1357396, 2024. doi: https://doi.org/10.3389/fbuil.2024.1357396.

[5] SHOJAEIFARD, M., BAGHANI, M., SHAHSAVARI, H., "Rutting investigation of asphalt pavement subjected to moving cyclic loads: an implicit viscoelastic-viscoplastic-viscodamage FE framework", *The International Journal of Pavement Engineering*, v. 21, n. 11, pp. 1393–1407, 2020. doi: https://doi.org/10.1080/10298436.2018.1546008.

[6] LIU, Z., GU, X., REN, H., "Rutting prediction of asphalt pavement with semi-rigid base: numerical modeling on laboratory to accelerated pavement testing", *Construction & Building Materials*, v. 375, pp. 130903, 2023. doi: https://doi.org/10.1016/j.conbuildmat.2023.130903.

[7] WANG, C., WANG, Z., "Prediction model for rutting of asphalt concrete pavement considering temperature influence", *Case Studies in Construction Materials*, v. 22, e04831, 2025. doi: https://doi.org/10.1016/j.cscm.2025.e04831.

[8] MUȘAT, E.C., BITIR, I., "Evaluating the forest road systems subjected to different loadings by using the Finite Element Method", *Forests*, v. 13, n. 11, pp. 1872, 2022. doi: https://doi.org/10.3390/f13111872.

[9] WANG, Y., GAO, Y., LI, B., *et al*., "One-way cyclic deformation behavior of natural soft clay under continuous principal stress rotation", *Soil and Foundation*, v. 57, n. 6, pp. 1002–1013, 2017. doi: https://doi.org/10.1016/j.sandf.2017.08.027.

[10] POWRIE, W., YANG, L.A., CLAYTON, C.R., "Stress changes in the ground below ballasted railway track during train passage", *Proceedings of the Institution of Mechanical Engineers. Part F, Journal of Rail and Rapid Transit*, v. 221, n. 2, pp. 247–262, 2007. doi: https://doi.org/10.1243/0954409JRRT95.

[11] DENG, Y., SHI, X., "Modeling the rutting performance of asphalt pavements: a review", *Journal of Infrastructure Preservation and Resilience*, v. 4, n. 1, pp. 17, 2023. doi: https://doi.org/10.1186/s43065-023-00082-9.

[12] YANG, C., HUANG, M.S., CUI, Y.J., "Constitutive model of unsaturated structured soils under cyclic loading", In: Alonso, E., Gens, A. (eds), *Unsaturated soils, two volume set*, 1 ed., London, CRC Press, pp. 987–992, 2010. doi: https://doi.org/10.1201/b10526-152.

[13] ALAMNIE, M.M., TADDESSE, E., HOFF, I., "Advances in permanent deformation modeling of asphalt concrete: a review", *Materials*, v. 15, n. 10, pp. 3480, 2022. doi: https://doi.org/10.3390/ma15103480. PubMed PMID: 35629508.

[14] AVINASH, N.R., VINAY, H.N., PRASAD, D., *et al*., "Performance evaluation of low volume flexible pavements-a case study", In: *T&DI Congress 2014: Planes, Trains, and Automobiles*, pp. 69-78, 2014. doi: https://doi.org/10.1061/9780784413586.007.

[15] HASAN, A.S., ROKSANA, K., KABIR, S.F., *et al*., "Investigation of typical distresses of flexible pavements in dhaka city and possible remedies", *International Journal of Pavement Research and Technology*, v. 28, pp. 1202–1227, 2025. doi: https://doi.org/10.1007/s42947-023-00409-5.

[16] FURLANI, E., TONELLO, G., MASCHIO, S., "Recycling of steel slag and glass cullet from energy saving lamps by fast firing production of ceramics", *Waste Management*, v. 30, n. 8-9, pp. 1714–1719, 2010. doi: https://doi.org/10.1016/j.wasman.2010.03.030. PubMed PMID: 20400283.

[17] MUGULA, J., NAKAYENGA, J., KIDO, R., *et al*., "Sustainable stabilization of sandy soils using steel slag and biopolymer cellulose", *Case Studies in Construction Materials*, v. 22, e04555, 2025. doi: https://doi.org/10.1016/j.cscm.2025.e04555.

[18] WANG, H.L., QIAN, J.S., LIU, J., *et al*., "Wear resistance analysis of steel slag aggregates based on morphology characteristics", *Construction & Building Materials*, v. 409, pp. 133649, 2023. doi: https://doi.org/10.1016/j.conbuildmat.2023.133649.

[19] CHEN, Z., WU, S., WEN, J., *et al*., "Utilization of gneiss coarse aggregate and steel slag fine aggregate in asphalt mixture", *Construction & Building Materials*, v. 93, pp. 911–918, 2015. doi: https://doi.org/10.1016/j.conbuildmat.2015.05.070.

(cc) BY

[20] LEI, B., YU, L., CHEN, J., *et al*.,"Sustainable asphalt mixtures reinforced with basic oxygen furnace steel slag: multi-scale analysis of enhanced interfacial bonding", *Case Studies in Construction Materials*, v. 22, e04198, 2025. doi: https://doi.org/10.1016/j.cscm.2024.e04198.

[21] KARADAG, H., FIRAT, S., ISIK, N.S., *et al*.,"Determination of permanent deformation of flexible pavements using finite element model", *Građevinar*, v. 74, n. 6, pp. 471–480, 2022. doi: https://doi.org/10.14256/JCE.2708.2019.

[22] ÖZSOY, M., FIRAT, S., "Numerical analysis of road layers made with steel slag", *Journal of Polytechnic*, v. 26, n. 4, pp. 1661–1673, 2023. doi: https://doi.org/10.2339/politeknik.1199022.

[23] ZHONG, T., ZHENG, Y., CHEN, Z., *et al*., "Utilization of steel slag as coarse aggregate and filler in stone mastic asphalt (SMA) mixture: engineering performance, environmental impact and economic benefits analysis", *Journal of Cleaner Production*, v. 450, pp. 141891, 2024. doi: https://doi.org/10.1016/j.jclepro.2024.141891.

[24] TOZZO, C., CHIOLA, D., PIERANI, M., *et al*., "Improving the EAR index for flexible pavement and a preliminary definition of an environmental index (ECR) for rigid pavement", *Construction Materials*, v. 4, n. 1, pp. 110–127, 2024. doi: https://doi.org/10.3390/constrmater4010007.

[25] TIMM, D.H., NEWCOMB, D.E., "Perpetual pavement design for flexible pavements in the US", *The International Journal of Pavement Engineering*, v. 7, n. 2, pp. 111–119, 2006. doi: https://doi.org/10.1080/10298430600619182.

[26] LADE, P.V., NELSON, R.B., "Modelling the elastic behaviour of granular materials", *International Journal for Numerical and Analytical Methods in Geomechanics*, v. 11, n. 5, pp. 521–542, 1987. doi: https://doi.org/10.1002/nag.1610110507.

[27] BRINKGREVE, R.B.J., BROERE, W. (eds), *Plaxis: 3D foundation. Version 1*, Leiden, Balkema, 2004.

[28] SHEN, K., WANG, H., "Prediction of critical strains of flexible pavement from traffic speed deflectometer measurements", *Construction & Building Materials*, v. 411, pp. 134770, 2024. doi: https://doi.org/10.1016/j.conbuildmat.2023.134770.

[29] ÖZSOY, M., "*Numerical analysis of road infrastructure with steel slag under statical and repeated loads*", D.Sc. Thesis, Gazi University, Ankara, 2023.

[30] LI, L., LING, T.C., PAN, S.Y., "Environmental benefit assessment of steel slag utilization and carbonation: a systematic review", *The Science of the Total Environment*, v. 806, n. Pt 1, pp. 150280, 2022. doi: https://doi.org/10.1016/j.scitotenv.2021.150280. PubMed PMID: 34560457.

[31] WORLD STEEL ASSOCIATION, *World steel in figures 2024*, https://worldsteel.org/data/world-steel-in-figures-2024/, accessed in January, 2025.

[32] BIRAT, J.P., "Sustainability footprint of steelmaking byproducts", *Ironmaking & Steelmaking*, v. 39, n. 4, pp. 270–277, 2012. doi: https://doi.org/10.1179/1743281211Y.0000000054.

[33] GUO, X., SHI, H., "Effects of steel slag admixture with GGBFS on performances of cement paste and mortar", *Advances in Cement Research*, v. 26, n. 2, pp. 93–100, 2014. doi: https://doi.org/10.1680/adcr.13.00003.

[34] FANG, M., FANG, G., XIA, Y., *et al*., "Study on compressive strength of concrete mixed by steel slag powder and fly ash", *IOP Conference Series: Earth and Environmental Science*, v. 508, n. 1, pp. 012183, 2020. doi: https://doi.org/10.1088/1755-1315/508/1/012183.

[35] CHEN, Z., LI, R., LIU, J., "Preparation and properties of carbonated steel slag used in cement cementitious materials", *Construction & Building Materials*, v. 283, pp. 122667, 2021. doi: https://doi.org/10.1016/j.conbuildmat.2021.122667.

[36] SONG, Q., GUO, M.Z., WANG, L., *et al*., "Use of steel slag as sustainable construction materials: a review of accelerated carbonation treatment", *Resources, Conservation and Recycling*, v. 173, pp. 105740, 2021. doi: https://doi.org/10.1016/j.resconrec.2021.105740.

[37] POH, H.Y., GHATAORA, G.S., GHAZIREH, N., "Soil stabilization using basic oxygen steel slag fines", *Journal of Materials in Civil Engineering*, v. 18, n. 2, pp. 229–240, 2006. doi: https://doi.org/10.1061/(ASCE)0899-1561(2006)18:2(229).

[38] NETINGER, I., BJEGOVIĆ, D., VRHOVAC, G., "Utilisation of steel slag as an aggregate in concrete", *Materials and Structures*, v. 44, n. 9, pp. 1565–1575, 2011. doi: https://doi.org/10.1617/s11527-011-9719-8.

[39] QASRAWI, H., "The use of steel slag aggregate to enhance the mechanical properties of recycled aggregate concrete and retain the environment", *Construction & Building Materials*, v. 54, pp. 298–304, 2014. doi: https://doi.org/10.1016/j.conbuildmat.2013.12.063.

[40] O'Connor, J., NGUYEN, T.B.T., HONEYANDS, T., *et al*., "Production, characterisation, utilisation, and beneficial soil application of steel slag: a review", *Journal of Hazardous Materials*, v. 419, pp. 126478, 2021. doi: https://doi.org/10.1016/j.jhazmat.2021.126478. PubMed PMID: 34323725.

[41] YI, H., XU, G., CHENG, H., *et al*., "An overview of utilization of steel slag", *Procedia Environmental Sciences*, v. 16, pp. 791–801, 2012. doi: https://doi.org/10.1016/j.proenv.2012.10.108.

[42] GAO, W., ZHOU, W., LYU, X., *et al*., "Comprehensive utilization of steel slag: a review", *Powder Technology*, v. 422, pp. 118449, 2023. doi: https://doi.org/10.1016/j.powtec.2023.118449.

[43] GU, L., DENG, X., ZHANG, M., *et al*., "Stabilization of fluidic silty sands with cement and steel slag", *Buildings*, v. 13, n. 11, pp. 2705, 2023. doi: https://doi.org/10.3390/buildings13112705.

[44] HOU, J., CHEN, Z., LIU, J., "Hydration activity and expansibility model for the RO phase in steel slag", *Metallurgical and Materials Transactions. B, Process Metallurgy and Materials Processing Science*, v. 51, n. 4, pp. 1697–1704, 2020. doi: https://doi.org/10.1007/s11663-020-01847-3.

[45] YUN, W., QU, X., MA, Z., *et al*., "Enhancing adhesion and performance of reclaimed asphalt mixtures using combined modified steel slag", *Journal of Adhesion Science and Technology*, v. 39, n. 7, pp. 1085–1104, 2025. doi: https://doi.org/10.1080/01694243.2024.2438164.

[46] JIANG, L., DONG, C.L., WANG, S.Y., "Reducing volume expansion of steel slag by using a surface hydrophobic waterproof structure", *Journal of Materials in Civil Engineering*, v. 32, n. 10, pp. 04020303, 2020 doi: https://doi.org/10.1061/(ASCE)MT.1943-5533.0003320.

[47] BRAND, A.S., FANIJO, E.O., "A review of the influence of steel furnace slag type on the properties of cementitious composites", *Applied Sciences*, v. 10, n. 22, pp. 8210, 2020. doi: https://doi.org/10.3390/app10228210.

[48] GOLI, H., LATIFI, M., SADEGHIAN, M., "Moisture characteristics of warm mix asphalt containing reclaimed asphalt pavement (RAP) or steel slag", *Materials and Structures*, v. 55, n. 2, pp. 53, 2022. doi: https://doi.org/10.1617/s11527-022-01893-0.

[49] KIM, D.H., SHIN, M.C., CHOI, H.D., *et al*., "Removal mechanisms of copper using steel-making slag: adsorption and precipitation", *Desalination*, v. 223, n. 1-3, pp. 283–289, 2008. doi: https://doi.org/10.1016/j.desal.2007.01.226.

[50] ABD EL-AZIM, H., SELEMAN, M.M.E.S., SAAD, E.M., "Applicability of water-spray electric arc furnace steel slag for removal of Cd and Mn ions from aqueous solutions and industrial wastewaters", *Journal of Environmental Chemical Engineering*, v. 7, n. 2, pp. 102915, 2019. doi: https://doi.org/10.1016/j.jece.2019.102915.

[51] LIN, S., ZHANG, T., CAO, X., *et al*., "Recovery of converter steel slag to prepare catalytic H_2O_2 degradation of dye wastewater as a catalyst", *Journal of Materials Science Materials in Electronics*, v. 32, n. 20, pp. 24889–24901, 2021. doi: https://doi.org/10.1007/s10854-021-06947-7.

[52] EUROSLAG, https://www.euroslag.com/products/statistics/statistics-2022/, accessed in January, 2025.

[53] KAVUSSI, A., JALILI QAZIZADEH, M., HASSANI, A., "Fatigue behavior analysis of asphalt mixes containing electric arc furnace (EAF) steel slag", *Journal of Rehabilitation in Civil Engineering*, v. 3, n. 1, pp. 74–86, 2015. doi: https://doi.org/10.22075/jrce.2016.364.

[54] BIBITHA, L., DURGALAKSHMI, S., ATHIAPPAN, K., "Evaluation of strength, wear, and skid resistance in pavement quality concrete with partial replacement of steel slag", *Matéria*, v. 30, e20240636, 2025. doi: https://doi.org/10.1590/1517-7076-rmat-2024-0636.

[55] PASETTO, M., BALIELLO, A., GIACOMELLO, G., *et al*., "Sustainable solutions for road pavements: a multi-scale characterization of warm mix asphalts containing steel slags", *Journal of Cleaner Production*, v. 166, pp. 835–843, 2017. doi: https://doi.org/10.1016/j.jclepro.2017.07.212.

[56] SCHWEIGER, H.F., "The role of advanced constitutive models in geotechnical engineering", *Geomechanik und Tunnelbau*, v. 1, n. 5, pp. 336–344, 2008. doi: https://doi.org/10.1002/geot.200800033.

[57] LITTLE, D.N., ALLEN, D.H., BHASIN, A., *et al*., "Failure mechanisms and methods to estimate material resistance to failure", In: Little, D.N., Allen, D.H., Bhasin, A. (eds), *Modeling and design of flexible pavements and materials*, Cham, Springer, pp. 283–338, 2018. doi: https://doi.org/10.1007/978-3-319-58443-0_8.

[58] PARJOKO, Y.H., "Sensitivity analysis of concrete performance using finite element approach", *Journal of the Civil Engineering Forum*, v. 21, n. 1, pp. 1171–1182, 2012. doi: https://doi.org/10.22146/jcef.18939.

[59] FANG, H., HADDOCK, J.E., WHITE, T.D., *et al*., "On the characterization of flexible pavement rutting using creep model-based finite element analysis", *Finite Elements in Analysis and Design*, v. 41, n. 1, pp. 49–73, 2004. doi: https://doi.org/10.1016/j.finel.2004.03.002.

[60] DENG, Y., LUO, X., ZHANG, Y., *et al*., "Evaluation of flexible pavement deterioration conditions using deflection profiles under moving loads", *Transportation Geotechnics*, v. 26, pp. 100434, 2021. doi: https://doi.org/10.1016/j.trgeo.2020.100434.

[61] ABU-FARSAKH, M.Y., GU, J., VOYIADJIS, G.Z., *et al*., "Mechanistic-empirical analysis of the results of finite element analysis on flexible pavement with geogrid base reinforcement", *The International Journal of Pavement Engineering*, v. 15, n. 9, pp. 786–798, 2014. doi: https://doi.org/10.1080/10298436.2014.893315.

[62] SHEN, K., ZHANG, H., TONG, J., *et al*., "Dynamic elastic analysis of flexible pavements under moving vehicles: a semi-analytical finite element treatment", *Road Materials and Pavement Design*, v. 23, n. 6, pp. 1440–1450, 2022. doi: https://doi.org/10.1080/14680629.2021.1883467.

[63] WANG, H., AL-QADI, I.L., "Combined effect of moving wheel loading and three-dimensional contact stresses on perpetual pavement responses", *Transportation Research Record: Journal of the Transportation Research Board*, v. 2095, n. 1, pp. 53–61, 2009. doi: https://doi.org/10.3141/2095-06.

[64] LEES, A., *Geotechnical finite element analysis: a practical guide*, London, ICE Publishing, 2016. doi: https://doi.org/10.1680/gfea.60876.

[65] TONG, J., MA, T., SHEN, K., *et al*., "A criterion of asphalt pavement rutting based on the thermal-visco-elastic-plastic model", *The International Journal of Pavement Engineering*, v. 23, n. 4, pp. 1134–1144, 2022. doi: https://doi.org/10.1080/10298436.2020.1792470.

[66] CHEN, B., ZHANG, X., YU, J., *et al*., "Impact of contact stress distribution on skid resistance of asphalt pavements", *Construction & Building Materials*, v. 133, pp. 330–339, 2017. doi: https://doi.org/10.1016/j.conbuildmat.2016.12.078.

[67] ZHENG, B., CHEN, J., ZHAO, R., *et al*., "Analysis of contact behaviour on patterned tire-asphalt pavement with 3-D FEM contact model", *The International Journal of Pavement Engineering*, v. 23, n. 2, pp. 171–186, 2022. doi: https://doi.org/10.1080/10298436.2020.1736294.

[68] GONG, Z., MIAO, Y., LANTIERI, C., "Review of research on tire-pavement contact behavior", *Coatings*, v. 14, n. 2, pp. 157, 2024. doi: https://doi.org/10.3390/coatings14020157.

[69] SIDDHARTHAN, R.V., KRISHNAMENON, N., EL-MOUSLY, M., *et al*., "Investigation of tire contact stress distributions on pavement response", *Journal of Transportation Engineering*, v. 128, n. 2, pp. 136–144, 2002. doi: https://doi.org/10.1061/(ASCE)0733-947X(2002)128:2(136).

[70] WANG, H., AL-QADI, I.L., STANCIULESCU, I., "Effect of surface friction on tire-pavement contact stresses during vehicle maneuvering", *Journal of Engineering Mechanics*, v. 140, n. 4, pp. 04014001, 2014. doi: https://doi.org/10.1061/(ASCE)EM.1943-7889.0000691.

[71] WOODWARD, D., MILLAR, P., LANTIERI, C., *et al*., "The wear of Stone Mastic Asphalt due to slow speed high stress simulated laboratory trafficking", *Construction & Building Materials*, v. 110, pp. 270–277, 2016. doi: https://doi.org/10.1016/j.conbuildmat.2016.02.031.

[72] PIDWERBESKY, B.D., "Strain response and performance of subgrades and flexible pavements under various loading conditions", *Transportation Research Record: Journal of the Transportation Research Board*, n. 1482, pp. 87, 1995.

[73] MUNIANDY, R., MOAZAMI, D., HAMID, H., *et al*., "Characterization of effective tire contact area for various tread patterns", *Instrumentation Science & Technology*, v. 42, n. 1, pp. 15–26, 2014. doi: https://doi.org/10.1080/10739149.2013.832291.

[74] WEISSMAN, S.L., "Influence of tire-pavement contact stress distribution on development of distress mechanisms in pavements", *Transportation Research Record: Journal of the Transportation Research Board*, v. 1655, n. 1, pp. 161–167, 1999. doi: https://doi.org/10.3141/1655-21.

[75] XIE, Y., YANG, Q., "Tyre-pavement contact stress distribution considering tyre types", *Road Materials and Pavement Design*, v. 20, n. 8, pp. 1899–1911, 2019. doi: https://doi.org/10.1080/14680629.2018.1473285.

[76] GHAEDNIA, H., WANG, X., SAHA, S., *et al*., "A review of elastic–plastic contact mechanics", *Applied Mechanics Reviews*, v. 69, n. 6, pp. 060804, 2017. doi: https://doi.org/10.1115/1.4038187.

[77] GUO, M., ZHOU, X., "Tire-pavement contact stress characteristics and critical slip ratio at multiple working conditions", *Advances in Materials Science and Engineering*, v. 2019, n. 1, pp. 5178516, 2019. doi: https://doi.org/10.1155/2019/5178516.

[78] PARK, D.W., FERNANDO, E., LEIDY, J., "Evaluation of predicted pavement response with measured tire contact stresses", *Transportation Research Record: Journal of the Transportation Research Board*, v. 1919, n. 1, pp. 160–170, 2005. doi: https://doi.org/10.1177/0361198105191900117.

[79] MOAZAMI, D., MUNIANDY, R., "Determination of relative damage of asphalt pavement from reduced tire contact area", *The International Journal of Pavement Engineering*, v. 19, n. 6, pp. 553–563, 2018. doi: https://doi.org/10.1080/10298436.2016.1178742.

[80] DE BEER, M., FISHER, C., JOOSTE, F.J., "Determination of pneumatic tyre/pavement interface contact stresses under moving loads and some effects on pavements with thin asphalt surfacing layers", In: *Proceedings of the 8th International Conference on Asphalt Pavements*, pp. 10–14, Lino Lakes, Minn., 1997.

[81] DE BEER, M., FISHER, C., "*Contact stresses of pneumatic tires measured with the Vehicle-Road Surface Pressure Transducer Array (VRSPTA) system for the University of California at Berkeley (UCB) and the Nevada Automotive Test Center (NATC)*, Berkeley, University of California, 1997.

[82] HUANG, Y.H., *Pavement analysis and design*. New Jersey, Pearson Prentice Hall, 2004.

[83] AL-QADI, I.L., LOULIZI, A., JANAJREH, I., *et al*., "Pavement response to dual tires and new wide-base tires at same tire pressure", *Transportation Research Record: Journal of the Transportation Research Board*, v. 1806, n. 1, pp. 38–47, 2002. doi: https://doi.org/10.3141/1806-05.

[84] WEISSMAN, S.L., "Influence of tire-pavement contact stress distribution on development of distress mechanisms in pavements", *Transportation Research Record: Journal of the Transportation Research Board*, v. 1655, n. 1, pp. 161–167, 1999. doi: https://doi.org/10.3141/1655-21.

[85] BARKSDALE, R.D., "Compressive stress pulse times in flexible pavements for use in dynamic testing", *Highway Research Record*, v. 345, n. 4, pp. 32–44, 1971.

[86] YOO, P.J., AL-QADI, I.L., ELSEIFI, M.A., *et al*., "Flexible pavement responses to different loading amplitudes considering layer interface condition and lateral shear forces", *The International Journal of Pavement Engineering*, v. 7, n. 1, pp. 73–86, 2006. doi: https://doi.org/10.1080/10298430500516074.

[87] SAAD, B., MITRI, H., POOROOSHASB, H., "3D FE analysis of flexible pavement with geosynthetic reinforcement", *Journal of Transportation Engineering*, v. 132, n. 5, pp. 402–415, 2006. doi: https://doi.org/10.1061/(ASCE)0733-947X(2006)132:5(402).

[88] ZHAO, X., ZHANG, Y., "Analyzing the mechanical and durability characteristics of steel slag-infused asphalt concrete in roadway construction", *Buildings*, v. 14, n. 3, pp. 679, 2024. doi: https://doi.org/10.3390/buildings14030679.

[89] YANG, C., WU, S., CUI, P., *et al*., "Performance characterization and enhancement mechanism of recycled asphalt mixtures involving high RAP content and steel slag", *Journal of Cleaner Production*, v. 336, pp. 130484, 2022. doi: https://doi.org/10.1016/j.jclepro.2022.130484.

[90] HUANG, X., YAN, F., GUO, R., *et al*., "Study on the performance of steel slag and its asphalt mixture with oxalic acid and water erosion", *Materials*, v. 15, n. 19, pp. 6642, 2022. doi: https://doi.org/10.3390/ma15196642. PubMed PMID: 36233989.

[91] YAO, D., YU, H., CHEN, X., *et al*., "Effect of surface modification on properties of steel slag aggregate and mixture", *Construction & Building Materials*, v. 402, pp. 133058, 2023. doi: https://doi.org/10.1016/j.conbuildmat.2023.133058.

[92] FANG, H., LIU, Q., MO, L., *et al*., "Characterization of three-stage rutting development of asphalt mixtures", *Construction & Building Materials*, v. 154, pp. 340–348, 2017. doi: https://doi.org/10.1016/j.conbuildmat.2017.07.222.

[93] CELAURO, C., "Influence of the hourly variation of temperature on the estimation of fatigue damage and rutting in flexible pavement design", *The International Journal of Pavement Engineering*, v. 5, n. 4, pp. 221–231, 2004. doi: https://doi.org/10.1080/10298430512331336592.

[94] FAHAD, M., NAGY, R., "Performance comparison of polymer and fiber modified asphalt mixtures", *Discover Applied Sciences*, v. 7, n. 6, pp. 570, 2025. doi: https://doi.org/10.1007/s42452-025-07134-7.

(cc) BY

[95] ZHU, Y., LI, Y., SI, C., *et al*., "Laboratory evaluation on performance of fiber-modified asphalt mixtures containing high percentage of RAP", *Advances in Civil Engineering*, v. 2020, n. 1, pp. 5713869, 2020. doi: https://doi.org/10.1155/2020/5713869.

[96] ZHU, C., LUO, H., TIAN, W., *et al*., "Investigation on fatigue performance of diatomite/basalt fiber composite modified asphalt mixture", *Polymers*, v. 14, n. 3, pp. 414, 2022. doi: https://doi.org/10.3390/polym14030414. PubMed PMID: 35160405.

[97] ANJU, M.J., BEULAH, M., VARGHESE, A., "Review of geopolymer composites synthesized using different industrial By-products", *International Journal of Pavement Research and Technology*, v. 19, n. 1, pp. 26–45, Jan. 2026. doi: https://doi.org/10.1007/s42947-024-00446-8.

[98] FAN, M., LYU, Z., LIU, L., *et al*., "Preparation of pavement base material by using steel slag powder and steel slag aggregate", *Matéria*, v. 29, n. 3, e20240257, 2024. doi: https://doi.org/10.1590/1517-7076-rmat-2024-0257.

[99] JWAIDA, Z., DULAIMI, A., MASHAAN, N., *et al*., "Geopolymers: the green alternative to traditional materials for engineering applications", *Infrastructures*, v. 8, n. 6, pp. 98, 2023. doi: https://doi.org/10.3390/infrastructures8060098.

[100] ANEKE, F.I., ONYELOWE, K.C., "Applications of preloading pressure on expansive subgrade treated with nano-geopolymer binder for cyclic crack resistance", *Nanotechnology for Environmental Engineering*, v. 7, n. 3, pp. 593–607, 2022. doi: https://doi.org/10.1007/s41204-022-00250-4.

[101] IKECHUKWU, A.F., MOSTAFA, M.M., "Assessing the coupling effects of nanosized fly ash and precompression stress towards mitigating subgrade cracks mobilised by traffic loading", *Nanotechnology for Environmental Engineering*, v. 6, n. 3, pp. 63, 2021. doi: https://doi.org/10.1007/s41204-021-00157-6.

[102] MARIYAPPAN, R., PALAMMAL, J.S., BALU, S., "Sustainable use of reclaimed asphalt pavement (RAP) in pavement applications: review", *Environmental Science and Pollution Research International*, v. 30, n. 16, pp. 45587–45606, 2023. doi: https://doi.org/10.1007/s11356-023-25847-3. PubMed PMID: 36820969.

[103] ONER, J., "Evaluation of mechanical properties for stone mastic asphalt containing textile waste", *Matéria*, v. 28, n. 2, e20230092, 2023. doi: https://doi.org/10.1590/1517-7076-rmat-2023-0092.